CHAPTER

7

IoT protocols, architectures, and applications

Chiara Buratti[a,b], Erik Ström[c,b], Luca Feltrin[d], Laurent Clavier[e], Gordana Gardašević[f], Thomas Blazek[g], Lazar Berbakov[h], Titus Constantin Balan[i], Luis Orozco-Barbosa[j], Carles Anton-Haro[k], Piotr Rajchowski[l], and Haibin Zhang[m]

[a] *University of Bologna, Bologna, Italy*
[c] *Chalmers University, Göteborg, Sweden*
[d] *Ericsson, Stockholm, Sweden*
[e] *Université de Lille, Lille, France*
[f] *University of Banja Luka, Banja Luka, Bosnia and Herzegovina*
[g] *Silicon Austria Labs, Linz, Austria*
[h] *Institute Mihailo Pupin, Belgrade, Serbia*
[i] *Universitatea Transilvania Braşov, Braşov, Romania*
[j] *Universidad de Castilla-La Mancha, Ciudad Real, Spain*
[k] *Centre Tecnològic de Telecomunicacions de Catalunya, Barcelona, Catalonia, Spain*
[l] *Gdańsk University of Technology, Gdańsk, Poland*
[m] *TNO, The Hague, Netherlands*

The proliferation of embedded systems, wireless technologies, and Internet protocols have enabled the IoT to bridge the gap between the virtual and physical world enabling the monitoring and control of the environment by data processing systems. IoT refers to the inter-networking of everyday objects that are equipped with sensing, computation, and communication capabilities. These networks can collaboratively interact and perform a variety of tasks autonomously.

A large variety of communication technologies has gradually emerged, reflecting a large diversity of application domains and requirements. This chapter describes some research activities performed with reference to such technologies and solutions. Section 7.1 reports the research in the framework of LPWANs, with emphasis on LoRa and Narrow Band IoT (NB-IoT) technologies. Studies on centralized approaches for IoT, mainly based on the IPv6 over the TSCH (6TiSCH) standard, are addressed in Section 7.2; while Section 7.3 deals with vehicular communications. Energy-efficient solutions are presented in Section 7.4, being energy consumption one of the main issues of IoT; Section 7.5 reports some architectural solutions for the

[b] Chapter editors.

Inclusive Radio Communications for 5G and Beyond. https://doi.org/10.1016/B978-0-12-820581-5.00013-4

application of the SDN and NFV paradigms to IoT. The chapter ends with research on specific applications and drawing some conclusions.

Most of the research described in the chapter has been conducted via experimentation, using testbeds described in IRACON White Paper on Experimental Facilities [AB18].

7.1 Low power wide area networks

The LPWAN technology has recently emerged specifically focusing on IoT applications which require low cost device, long battery life time, small amounts of data exchanged and long distances to be covered. The key features of LPWANs can be summarized as follows: (i) wide area coverage (up to some tenths of kilometers), (ii) low cost communication, (iii) long battery life (up to 10 years), and (iv) low bandwidth communication. Among these technologies, LoRa and NB-IoT are those supported by many network operators and have been investigated in many research works. This section discusses the achieved results, possible improvements of these technologies and some real applications which may benefit from their use.

7.1.1 LoRaWAN

LoRaWAN is one of the first technologies defined for LPWAN applications. Its standardization was initiated by Semtech, an American company which owns the patent for the synthesizer used to generate the modulated signal, and later by the LoRa Alliance, an organization of many companies which shared the effort to define a new standard for these new applications.

Two independent studies aimed to characterize the link layer performance of LoRa modulation. In [FMB+16,FBV+18] two Semtech SX1272 modules were deployed at increasing distances and in LOS conditions, one module was on a 240 m high hill in Bologna and the other one, the transmitter, was deployed in different locations up to 10.8 km far from the receiver, the maximum distance reached in this experiment.

In [CLC+19], the ranging capabilities of LoRa modulation are evaluated in three distinct environments, i.e., coastal, forest, and urban with antennas at 1.5 m height. The SNR is boosted by increasing the Spreading Factor (SF). In addition to improving the SNR, the sensitivity is increased yielding a higher link budget. However, transmitting with a higher SF will not result in a higher Received Signal Strength (RSS). Hence, the SNR does not decrease to the same degree as the RSS, with increased distance. Even in the urban scenario, a good average SNR, w.r.t. the demodulation floor, is measured despite the low received signal strength. The experimental results indicate that the range is mainly limited by the SNR demodulation floor rather than the RSS. The transmit power, coding rate, spreading factor, and other parameters will determine the maximum coverage. The measurements show that the SNR sensitivity

is reached before the RSS sensitivity for SF equal to 12. This confirms that the range is constrained by the SNR.

In [FMB+16,FBV+18] the orthogonality among transmissions with different SF was checked. Two devices transmitted simultaneously packets containing independent payload and using different SF. The packet success rate (P_s) was estimated by counting the number of received packets, while the Signal-to-Interference (SIR) was measured with a spectrum analyzer. In terms of capture ratio, defined as the minimum SIR allowing to guarantee a success rate of 50%, the experiment shows that when the SF of the two transmissions is the same it ranges between 1 and 2 dB, whereas when the SF of the two transmissions is different it ranges between -10 and -30 dB. This demonstrates that transmissions with different SF are not perfectly orthogonal, but in some cases the interference of concurrent transmissions should be taken into account.

In [FBV+18] the performance of a large network was evaluated through simulations, considering a square area with the LoRa Gateway (GW) located in the center and a variable number of nodes uniformly deployed. The network capacity is computed as the maximum number of packets per unit of time that a LoRa GW is able to process while guaranteeing a packet error rate lower than 10%. Fig. 7.1 (left) shows how the packet success rate changes when the offered traffic increases in a square area of 1 km^2, where all nodes can reach the gateway using any SF, and when 200 bytes of application data are transmitted. Different curves represent different settings of initial SF,[1] when using Acknowledgment packets and retransmissions (Confirmed) and when not (Unconfirmed). The simulations show that in case of a small area to cover, the best solution is to set SF equal to 7, in order to avoid collisions by keeping the packet time-on-air as small as possible. Moreover, when there is not much traffic in the network, the confirmed mode is the best choice to guarantee a high success rate; while when the network is more congested, retransmissions increase the collision probability. In this scenario a single GW is able to process up to 1.71 packets/s. Fig. 7.1 (right) shows how the packet success rate varies when the offered traffic increases in a larger area (46.5 km^2), where it is not possible to cover all devices with SF equal to 7 and only one GW. To overcome the coverage issue two solutions are represented in the figure, letting the device increase their SF when a confirmed message has not been acknowledged, or increasing the number of GWs deployed in the area avoiding confirmed transmissions. In the first case, the radio channel is utilized more intensively due to longer packet duration, a behavior that can lead quickly to the saturation of the network. The resulting network capacity is 0.46 packets/s. In the latter case, more GWs need to be deployed, but the average SF used by the devices, and thus the packet duration, is lower causing less collisions. The resulting capacity is 17.4 packets/s.

Some research has been devoted to possible enhancements of the LoRa technology [NCB18]. To limit the negative effect of collisions between transmissions performed with the same SF a solution is to utilize Successive Interference Cancella-

[1] SF is increased by one every two retransmissions.

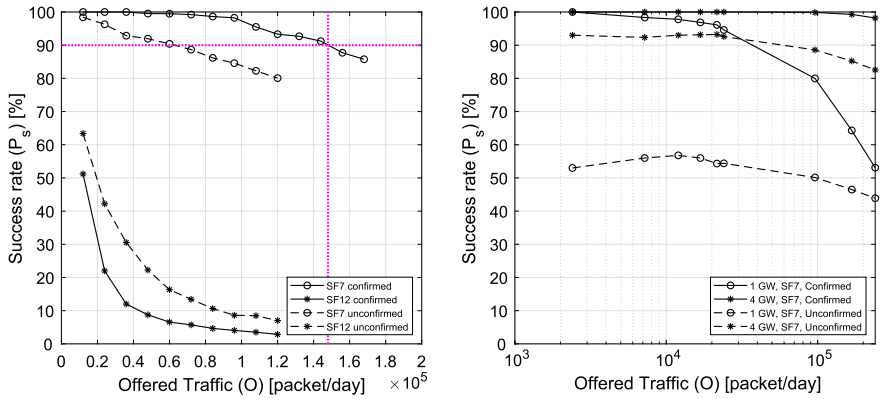

FIGURE 7.1

Packet Success Rate in a LoRaWAN network: One GW small area (left), Multiple GWs and large area (right).

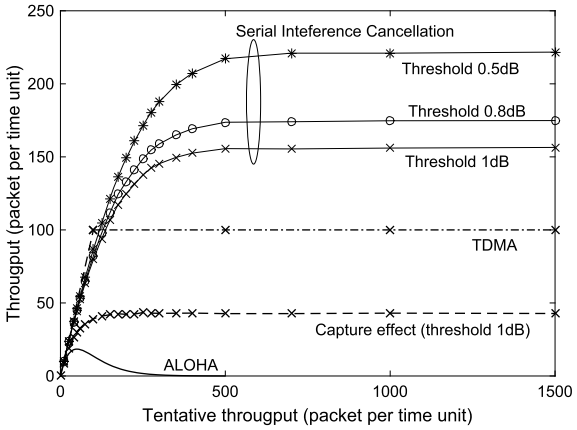

FIGURE 7.2

Performance comparison among different techniques employed to overcome collisions in LoRa.

tion (SIC), which is widely studied as a technique to enable receivers to demodulate multiple signals from their received sum. Fig. 7.2 shows the throughput of a LoRa based system affected by collisions as the network size, N, increases. The assumption is that all the nodes are using same SF and their packet generation rate is the maximum allowed by regional duty cycle limitations. It can be observed that SIC can significantly improve the network performance. This case study is in the sense of worst case scenario because no channel coding is used which would significantly improve the performance.

7.1.2 NB-IoT

NB-IoT is an access technology defined by 3GPP for massive Machine Type Communication (mMTC). NB-IoT implements several mMTC-oriented enhancements compared to other mobile technologies. Examples are: *(i)* narrow-band transmission and the exploitation of repetitions to reach devices in challenging positions such as basements or underground; *(ii)* differentiation of UE performance according to coverage areas by tuning parameters of the physical channels and network procedures; *(iii)* enhanced power saving mechanisms to improve the battery life; *(iv)* simplification of network procedures to reduce the UE complexity.

In [FCM+18,FMPV17], the main characteristics of the technology are presented together with a mathematical model representing the network performance of a NB-IoT cell composed of multiple devices in different coverage conditions, transmitting small packets to the network. In a typical dense urban scenario, like the city of London, the eNBs are placed in an hexagonal grid with a variable Inter-Site Distance (ISD) each of them forming a three-sectorial site. The main network configuration parameters taken into account are the number of preambles per second available in each coverage class NB-IoT Physical Random Access Channel (NPRACH) channel (Z_c), the number of repetitions used in each physical channel (R_c, for simplicity common to all the channels), and the thresholds to determine in which coverage class each device belongs to based on the received power from the eNB (Th_c). The study aims to find the configuration which maximizes certain performance metrics. In general the model can be adapted to consider different performance targets, in this case the optimal configuration maximizes the network throughput provided that the success probability is more than 90%. This is achieved by generating random configurations and assessing the resulting network performance. Fig. 7.3 shows the result of this evaluation with ISD = 1732 m (left) and ISD = 3464 m (right) where each point represents the resulting performance in a given configuration. With ISD = 1732 m the maximum throughput achievable is 52.4 kbps with a success rate of 96%. In this scenario the devices are split mostly in only two coverage classes with 1 and 2 repetitions respectively. A third class configured with 1 repetition is mostly unused showing that it is not needed, as coverage is not a major issue. Indeed, operators may decide to switch off the dedicated NPRACH in order to gain more resources for the NB-IoT Physical Uplink Shared Channel (NPUSCH) and accommodate more user data. With ISD = 3464 m the maximum throughput achievable drops to 10.4 kbps, but in this case the three coverage classes are configured with 1, 4, and 16 repetitions respectively and the devices are distributed evenly among them. In this scenario coverage is an issue that NB-IoT can solve by using the coverage classes concept and enabling a higher number of repetitions.

In [MPLC16] it is studied the possibility to enable mMTC applications by sharing the UHF spectrum with DTT. The proposed scenario considers a DVB-T2 network offering fixed rooftop reception as a primary service and NB-IoT network as a secondary service allocated to DTT white spaces. The results indicate that it is not feasible to allocate the NB-IoT carrier within the DVB-T2 channel, because of low power (between -38 and -36 dBm) that could transmit the small cell without interfer-

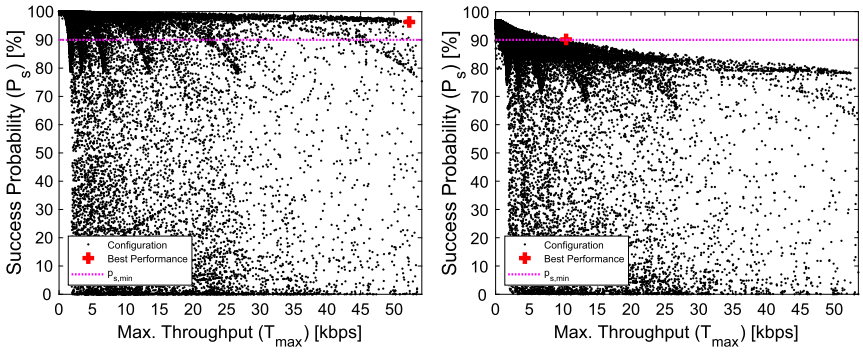

FIGURE 7.3

Random configurations of a NB-IoT network and best performance.

ing with the DVB-T2 channel. The NB-IoT small cell could transmit up to 15 dBm for adjacent channel with a 1 MHz guard band and there is no angular antenna discrimination. If it is considered, the improvement in the EIRP will be equivalent to the antenna discrimination (16 dB). The maximum allowable EIRP that the IoT devices can transmit varies between 9 and 14 dBm for the best case (Smart Parking) with a 2 MHz guard band. For the most restrictive case (Traffic Congestion) it is possible to transmit between 3 and 8 dBm with the same guard band, being this power enough to ensure a right operation.

In [FTC+19] it is considered another important scenario for mMTC communication, that is over-the-air firmware update. Given the presence of many devices per cell, a simple unicast update of the firmware generates a considerable amount of traffic which should be processed properly in order to avoid network saturation. In this work the transmission of one MBytes of firmware data is required in presence of normal application traffic. The performance using unicast transmission is compared to the one using Single Cell Point-to-Multipoint (SC-PTM), a feature introduced in Rel-14 of NB-IoT standard to enable multicast communication. The gains in terms of delivery time introduced by SC-PTM are quite obvious w.r.t. unicast. For unicast mode the delivery time varies from the order of hours to 1 day when increasing the ISD from 500 m to 1732 m, while it varies from the order of minutes to 1 hour for the SC-PTM. This indicates that the effective gains of SC-PTM w.r.t. unicast mode are strictly related to the location of UE. Nevertheless, it is worth emphasizing that while the delivery time is affected by the number of UE in the unicast case, the SC-PTM has a performance that does not vary with the number of UE being served. Thus, the choice of using either unicast or SC-PTM depends on the number of UE to be served and their coverage class.

A particular focus was given to Smart Grids application, which represent one of the target use cases that steered most the NB-IoT development.

In [PCF17] connectivity evaluations have been performed considering typical Smart Grid Wide Area Network (WAN) use cases in a real geographical zone of Italy

(Parma area), where Smart Meters can be deployed in different locations: outdoor, when the smart meter is located outside the building, indoor, when the meter is located in a propagation attenuation environment such as the first floor of the building, and deep indoor, when the meter is located in a deep propagation attenuation environment such as the basement of the building. The coverage evaluation were performed for both NB-IoT and LoRaWAN technologies assuming the same sites number and sites locations to enable a suitable comparison among the proposed solutions. Also it has to be considered both a single Mobile Network Operator (MNO) scenario and a roaming scenario. The evaluation highlights that the maximum percentage of uncovered area falls in the rural areas; indeed, considering only LTE sites, more than 40% of the rural areas is not covered by LoRaWAN, whereas 10% is not covered by NB-IoT.

In [NLZ18] various scheduling designs are compared with the aim of maximizing the transmission reliability. Use cases in the distribution segment include (on demand or periodic) remote meter reading, Real Time Pricing (RTP), and Object Relational Mapping (ORM). In the study ORM is considered to be the most demanding use case for the presented suitability assessment of NB-IoT technology in smart grids, meter reading is considered as background traffic. The network generally consists of a ring of substations (converting medium to low voltage), from where distribution feeders originate in a radial topology towards multiple households, each with a smart meter installed. The scheduler combining Earliest Due Date First and Shortest Processing Time First prioritization with Maximum Granularity Allocation subcarrier allocation achieves the highest reliability for nearly all outage percentages. We see a performance degradation as the granularity of the UL subcarrier allocation decreases (from Maximum Granularity Allocation to Least Granularity Allocation). Thus, due to the small packet sizes involved, increasing the granularity helps to decrease the waiting time of UEs which improves both the success rate and the 95th transfer delay percentile.

7.2 MAC and routing protocols for IoT

The design of efficient MAC and routing protocols in WSNs and IoT has been investigated for many years, with particular attention to design of distributed algorithms. However, some emerging applications, such as Industrial IoT (IIoT), are imposing strict requirements in terms of data transmission reliability, energy efficiency, throughput, and delay bounds, which cannot always be guaranteed by distributed solutions, like IEEE 802.15.4/Zigbee. Such applications demand new approaches to IoT protocols design, based on centralized solutions, where a central entity has a complete view of the network's characteristics and requirements, thus being able to compute a global schedule and paths. 6TiSCH is an example of centralized network and scheduling solution, aiming at providing deterministic and latency-bounded wireless communications.

This section presents main results of research activities related to centralized solutions, based on the IEEE 802.15.4e/6TiSCH protocol stack. One activity was devoted to the definition and experimental testing of a joint scheduling and routing protocol, while another one was dealing with the definition and testing of an energy-efficient routing protocol. The section concludes with a description of congestion control algorithm for IoT networks.

7.2.1 6TiSCH protocol stack

Time-Slotted Channel Hopping (TSCH) is a synchronous MAC protocol introduced in IEEE 802.15.4e [TSC12], as a recent amendment to the IEEE 802.15.4 standard [80211]. In TSCH network, channel hopping is used, while the superframe concept defined in IEEE 802.15.4 has been replaced by the concept of slotframes. A slotframe consists of a matrix of cells and each cell is defined by a pair of time slot (typically 10 ms) and channel offset. TSCH defines two types of cells: dedicated and shared. A dedicated cell is contention-free providing that only one transmitter can send a packet. If cells are shared among multiple nodes, TSCH defines a back-off algorithm to avoid the contention. One of possible scheduling approaches is that the overall communication is orchestrated by a centralized entity/controller. This entity (usually denoted as coordinator or sink) defines the action (transmit, receive, sleep) performed by each node in each time slot. The combination of time synchronization and channel hopping in IEEE 802.15.4e provides the reliable and efficient communication, which is robust against external interference and persistent multi-path fading. The 6TiSCH protocol stack [Thu18] presents the IEEE 802.15.4 standard at physical layer, TSCH at MAC layer, 6top for adding/deleting TSCH slots between neighboring nodes, IPv6 over Low-Power Wireless Personal Area Network (6LoWPAN) to adapt the transmission of Internet Protocol version 6 (IPv6) frames over TSCH, and Routing Protocol for Low-Power and Lossy Networks (RPL) as a proactive dynamic routing protocol (see Fig. 7.4).

OpenWSN[2] is an open-source implementation of the protocol stack shown in Fig. 7.4. In [VG16] an in-depth performance evaluation of this protocols stack using OpenMote-CC2538 devices[3] has been provided and further results can be found also in [GVV16]. Moreover, in [GPV19] Authors provide some preliminary results of an experimental campaign, aiming at better understanding the mechanisms of the scheduling and routing in 6TiSCH networks. The paper shows that a proper selection of 6TiSCH configuration parameters and synchronization mechanisms is needed for a stable and optimal coexistence of 6TiSCH and RPL protocols. This campaign was conducted using a new board, OpenMote-B, designed primarily for IIoT applications. OpenMote-B is a dual-band device allowing communications using 2.4 GHz, as well as 868 MHz, it is the first board that fully supports the IEEE 802.15.4g standard including MR-OFDM modulations for robust communications. [SGV18] presents

[2] See http://www.openwsn.org/.
[3] See https://www.openmote.com/.

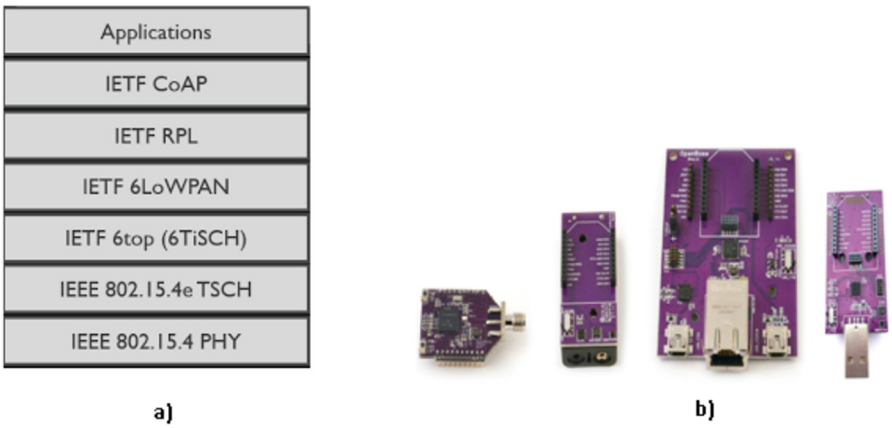

FIGURE 7.4

a) 6TiSCH Protocol Stack; b) OpenMote devices.

initial steps in porting RIOT[4] Operating System (OS) to OpenMote-B hardware platform.

7.2.2 Joint scheduling and routing protocols

The IEEE 802.15.4e standard does not specify details of the TSCH scheduling and resource allocation mechanisms, thus leaving many aspects to protocol designers. To bridge this gap, in [GVBV18] it was designed a Joint Scheduling and Routing Algorithm (JSRA), implemented on top of IEEE 802.15.4e. The algorithm jointly defines the set of paths connecting each node to the sink and the set of time slots they have to use for the communication (please, refer to [BV18b] for more details). Similarly to the Dijkstra's algorithm, which builds the tree iteratively by progressing from the root, at each iteration when a new link is added to the tree, a time slot is assigned according to the actual interference generated on the previously defined links. This ensures that packet losses are avoided, since the SIR (accounting for the sum of all possible interference) is kept above the capture ratio for all links.

As a second step, the JSRA algorithm has been integrated into the 6TiSCH protocol stack and implemented on the OpenMote-CC2538 platform. The testbed consists of ten nodes located into boxes on the walls of a corridor at the University of Bologna. Results, reported in Table 7.1, show the packet delivery ratio and throughput obtained by JSRA and 6TiSCH protocols. JSRA outperforms the standard solution in terms of throughput due to the possibility to assign the same slot to different links (see Fig. 7.5, where an example of routing and the scheduling outcomes for JSRA is shown), at the cost of a decreasing of the packet delivery ratio of 1%.

[4] See https://riot-os.org/.

Table 7.1 Comparison of JSRA and 6TiSCH protocols.

Protocol	Packet Delivery Ratio	Throughput [kbps]
6TiSCH	100%	12
JSRA	99%	15

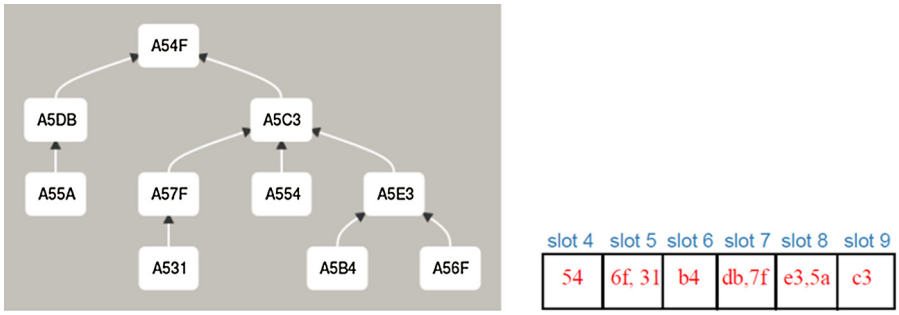

FIGURE 7.5

a) Routing topology obtained by JSRA and b) Scheduling obtained by JSRA.

Specific scheduling issues and challenges in 6TiSCH networks were also addressed in [GV18]. In this work a 6TiSCH simulator is used to demonstrate the performance of On-The-Fly (OTF) scheduling. The OTF algorithm is a distributed strategy for adapting the scheduled bandwidth to network requirements. The node negotiates the number of cells scheduled with its neighbors, without the intervention of a centralized entity. This report provides the simulation analysis based on various parameters including TSCH, RPL, OTF parameters, radio and propagation parameters, number of nodes and channels, node allocation area and deployment constrains, in order to measure performance, such as, End-to-End (E2E) reliability, E2E latency, the number of scheduled slots, etc. Simulation results show that OTF may achieve an E2E reliability up to 99%.

7.2.3 Routing protocols and congestion control

Routing in IoT networks has been extensively studied in the last decade, with the aim of reducing as much as possible the energy consumption, to increase the lifetime of battery-driven sensor nodes.

Authors in [DFGTV17] present a novel protocol, that is the combination of Source Routing (SR) and Minimum Cost Forwarding (MCF) protocols, which aims at reducing the energy consumption by communicating over paths with minimum cost. Source Routing for Minimum Cost Forwarding (SRMCF) is a reactive protocol, where nodes acquire routes on-demand and avoid saving information about the network topology. No information about the network topology is kept at nodes, but nodes always communicate over paths with minimum cost, independently of the traffic type. SRMCF has been implemented on Telos-B motes and experimental results in

a real scenario has been performed over a small network, to compare SRMCF to MCF protocol. Results show that the proposed solution presents a 33% higher throughput and 24% less energy consumption than MCF. The impact of using SRMCF with two different MAC protocols, Berkeley-MAC and Contiki-MAC, has been also evaluated via simulations.

[DGGV17] aims at applying the SRMCF routing protocol into the IIoT context. In particular, the SRMCF protocol has been integrated into the 6TiSCH OpenWSN protocol stack and implemented on OpenMote-B devices. Preliminary results of this research are reported in [RVG18,RVG19], where the SRMCF protocol has been compared to RPL. An example of results is reported in Fig. 7.6, where it is shown the Round Trip Time (RTT) for the two protocols, defined as the time between the generation of a query at the sink, to be transmitted (via multi-hopping) to a specific node in the network, and the instant in which the reply, generated by the node, reaches the sink. The RTT is shown by varying the number of hops separating the sink and the node, and the payload size of the query/reply packets. From the results it is possible to observe the effects of slot frame size upon the performance of the protocol and how higher payload sizes generate higher values of RTT as the number of hops increases, mainly due to queue overflow at relays.

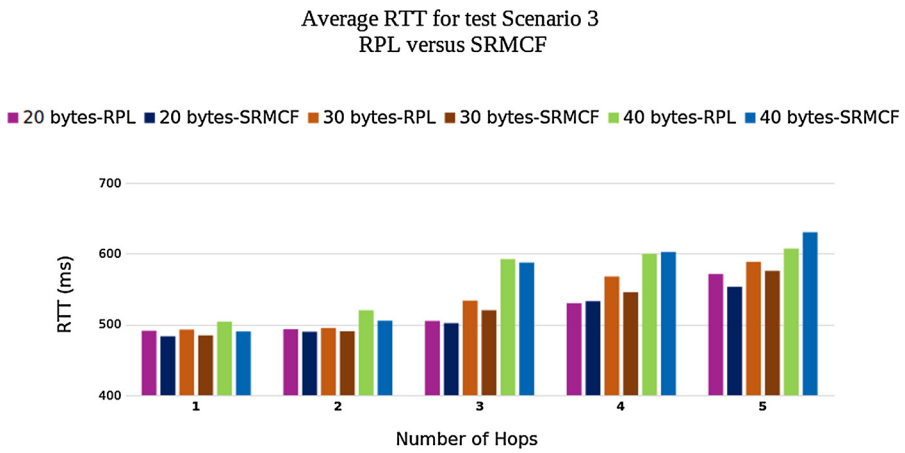

FIGURE 7.6

Average RTT as a function of the number of hops for RPL and SRMCF [RVG19].

We conclude this section addressing another important issues in IoT networks, that is related to traffic congestion, happening when a huge amount of information generated by different nodes needs to be transferred towards a single sink. Indeed, in case of congestion nodes queues may overflow and packets may be randomly dropped. As a consequence, valuable information can be lost on its way to the sink. To avoid this phenomenon, the network should be able either to avoid entering this state or to identify the congestion and recover (self-heal) in order to prevent loosing valuable information. Authors in [TSVG17] present a solution in which mobile

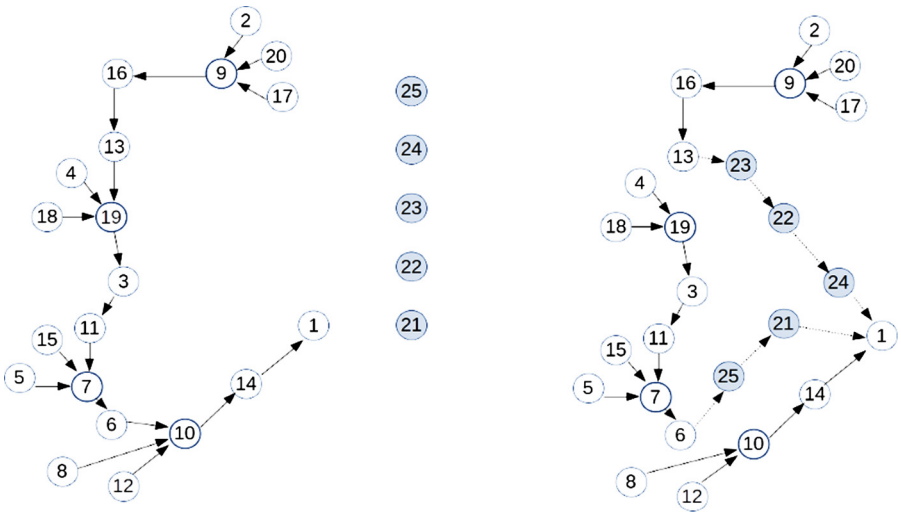

FIGURE 7.7

(a) Topology at congestion detection before Mobile-CC and (b) Topology after Mobile-CC node placement [TSVG17].

nodes are used to control and alleviate congestion and other impairments. In particular, they present a mechanism, denoted as Mobile-Congestion Control (CC), that can run above existing congestion control algorithms and employ mobile nodes in order to either create locally significant alternative paths towards the sink or generate direct paths of mobile nodes to the sink (see Fig. 7.7). A distributed congestion detection mechanism is also defined, such as a mechanism for deciding which nodes could not be used anymore as relays, because they are detected as congested. Simulation results show that the solution can significantly contribute in the alleviation of congestion in IoT. The same technique can be used to recover from other types of network faults as well.

7.3 Vehicular communications

The topic of vehicular communications has seen two main focus points. On the one hand, antenna design for V2X communications has been studied. This includes antenna types, patterns and MIMO deployments. Furthermore, the topic of antenna placement in recessed roof cavities has been researched. On the other hand, the topic of performance estimation and analysis in a new, highly dynamic environment was a strong focus. This included measurement campaigns as well as stochastic modeling approaches, and hybrid designs including hardware emulation and system level simulations. Both vehicular ad-hoc networks, as well as train communications were

the focus of the analysis. In the following sections, the work of the two topics is presented.

7.3.1 Antenna design and integration

Applications in the IoT are usually thought of as small devices like sensor networks, but large vehicles such as trains and cars are now rethought as connected devices in the IoT. These connected vehicles can access infotainment via the IoT and share safety critical information directly by establishing ad-hoc networks. Thereby, vehicles become more communicative, which increases the demand for vehicular antennas. Especially, the exchange of safety related information requires reliable and redundant wireless communication. In principle automotive antennas should provide omnidirectional coverage, as the orientation of the car towards other stations will in general be unknown beforehand. However, once communication with a specific partner is established, it is desirable to have increased antenna gain towards this direction, e.g. by beam-steering.

Some research has been devoted to investigate the possibility to flush-mount pattern reconfigurable antennas inside chassis antenna cavities, see Fig. 7.8. Five pattern reconfigurable antennas were measured inside a chassis antenna cavity [AKMZ17a,AKMZ17b,AKMZ19].

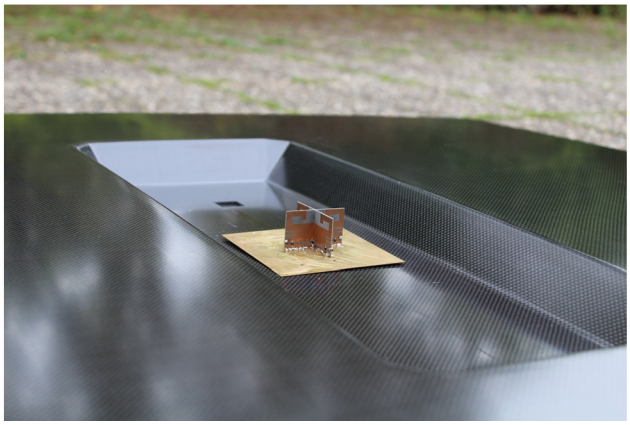

FIGURE 7.8

An antenna that can be reconfigured between four directions [AKMZ17b] is flush-mounted inside a chassis antenna cavity prototype made from carbon fiber reinforced polymer.

[AKMZ17a] compares the performance of three antennas that are reconfigurable between a front/back and a left/right state. All three antennas are built with two driven elements that can be switched to radiate in phase or with a 180° phase shift, but the antennas differ in the design of their radiating elements and switching mechanisms. Quarter-wavelength monopole antennas, inverted-L antennas and inverted-F antennas are explored as driven elements. It is shown that the antennas retain their reconfigura-

tion capabilities when they are flush-mounted. Further, measurements show that such antennas can be designed with various switched gain differences, e.g. to reconfigure between states that are both quasi-omnidirectional and can provide a few additional decibel of antenna gain, or with large gain differences around 20 dB to reduce interference from vehicles in the front.

[AKMZ17b] prototypes and measures a flush-mounted antenna that can be reconfigured between four directions, e.g., front, back, left, and right. Such antennas can be used to selective transmit safety critical information in traffic. For example, a car that plans to change lanes on a highway can broadcast a message with increased gain towards its right side before starting to swerve. [AKMZ19] demonstrates an automotive antenna that can be hidden in a cavity and that is reconfigurable in 45°-steps towards eight directions. The antenna is designed as electronically steered parasitic array radiator and allows even finer beam-steering.

New concepts for automotive antennas have been explored in [GKDGH18], presenting a prototype of an antenna cavity that is built into the roof above the windshield. This concept is opposed to state-of-the-art shark-fin antenna modules that are located at the rear roof end. Measurements show that antennas at this location offer increased coverage towards low elevation angles in front of the car, which is paramount for communication with vulnerable road users.

FIGURE 7.9

An automotive antenna roof [AKGH] is prototyped and measured inside the anechoic chamber at VISTA, TU Ilmenau, Germany.

[AKGH] takes this concept a step further and proposes to use the whole car roof for antennas. Three antenna modules are introduced for flush-mounted antennas: A cavity above the windshield, a cavity in the roof center, and an antenna shelf at the rear roof end which elevates the antennas inside shark-fin modules to decrease shadowing from the roof curvature, see Fig. 7.9. The performed measurements show that quasi-omnidirectional coverage is possible from all three locations and that the increased distance between antennas increases the MIMO performance by lowering the correlation.

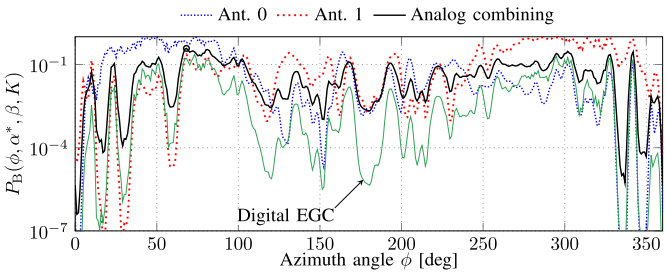

FIGURE 7.10

Burst error probability of using a single antenna (Ant. 0 or Ant. 1) compared with the proposed analog combining. As a reference, digital equal-gain combining (EGC) performance is also plotted.

A different take at robustness of the antenna patterns is shown in [NSB+18]. Here, the goal is to use L non-ideal antennas that can be purchased at low cost, and combine them in an efficient way to avoid error bursts due to bad antenna patterns. Crucially, the combination happens before the receiver, so that only one receiver is required. The authors choose minimizing the probability of error bursts as figure of merit, and aim to minimize the probability that K consecutive packets arriving from the worst-case angle-of-arrival are decoded incorrectly. To minimize complexity, the combining network does not estimate or use channel state information (complex channel gains, noise levels, etc.). The combining network consists of $L - 1$ analog phase shifters whose phases are affine functions of time. For a general L and the case when the packet error probability decays exponentially with the received SNR, the optimum slopes of the affine functions can be computed by solving an optimization problem that depends on the antenna far field functions. The authors provide an analytical solution for the special case of $L = 2$ antennas, which turns out to be independent of the antenna patterns. In an experimental setup consisting of two monopole antennas mounted on the roof of a Volvo XC90, the proposed combining method is shown to give significant performance gains compared to using just one of the antennas, see Fig. 7.10.

7.3.2 High mobility performance analysis and modeling

High mobility applications pose new challenges to the quality and reliability of data communications. The unique challenges of the outdoor channel with large delay spreads, coupled with the broad Doppler spectra associated with high mobility applications require thorough analysis of achievable data rates and latency. The full spectrum of tools has been employed to capture these conditions and move network connectivity analysis closer to reality.

The first presented problem is the coverage and throughput challenge associated with high speed trains. [BSOM17] presents two solutions to address this problem in cellular network services: On the one hand, amplify-and-forward Moving Relay

Nodes (MRNs) are studied. Furthermore, prototype windows are applied on on-board Wi-Fi enabled High Speed Trains (HSTs). The presented work applies the framework of hypothesis testing to extensive penetration loss and throughput tests. The tests are conducted with 3G/4G UEs located on-board the vehicles traveling throughout long-range geographical routes. This work is supported by real-world measurements conducted along Austrian railways such as from Vienna to Salzburg and from Vienna to Graz. The results are presented under the name SegHyPer, which works on route segmentation link quality parameters to enable micro-analysis in current and future cellular networks for mobile users on-board railjet HST.

In [BM18], the authors use vehicular highway throughput measurements such as the previous presented ones, and use them to estimate performance models. However, the focus of the work does not lie on throughput alone. Instead, the authors consider safety critical applications, where the burst properties of the transmission errors are just as important to estimate as the mean packet error rate. The presented approach takes its inspiration from the Gilbert-Elliot model, a two-state Markov chain. The model parameters are allowed to change to account for the non-stationarity of the channel. Based on this, maximum likelihood formulations for the model states are introduced. These formulations are then specified to estimate two different models. One model is parametrized on the measured 1-second mean SNR and uses the Baum-Welch algorithm to deduce the model parameters from recorded packet traces (called the mean SNR grouped estimator). The other approach takes the measured momentary SNR, and correlates it with packet loss events. This is used to estimate a momentary SNR threshold above which the packet will be transmitted successfully (the fading aware estimator). The results demonstrate that capturing the burst properties is essential, as the probability of burst errors is continuously high throughout the SNR range.

The previous work considered in-detail modeling of single link packet performance. However, in dense environments, the bulk of packet loss can be expected due to interference of neighboring nodes. This is the focus of [BBG+19]. Here, the goal is to use network simulations of dense city traffic, and analyze the resulting stochastic properties. To this end, SUMO is used as mobility simulator with a map of the city of Pristina in Kosovo. The resulting positions are used in OMNET++ with the VEINS extension, to generate VANET packet traffic. The traffic parameters are set to 10 packets per second and vehicle, with either 200 or 500 byte packets. The authors investigate the joint probabilities of number of neighbors in communication range and resulting packet loss due to hidden node interference. The first results show, that typical simple assumptions, such as Poisson Point Processes and Manhattan Grids do not reflect the results of the simulation. Hence, better assumptions are needed. Furthermore, the authors provide an estimate for the packet loss PDF due to interference, parameterized over the number of neighbors using the Gamma distribution. A similar analysis was carried out by the authors in [BLA+ed]. There, the Gilbert-Elliott approach for the single link was combined with the interference simulation approach, to evaluate an overall packet error probability. The result is shown in Fig. 7.11. The authors show that both aspects are equally important in this setting.

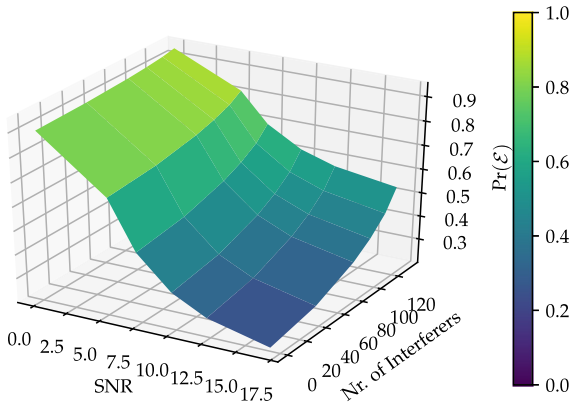

FIGURE 7.11

Combined packet error probability from single link analysis and interference modeling.

In these works, network simulators play an integral role for studying and evaluating vehicular communications. However, analysis is required on the accuracy of such simulations. An analysis on this has been conducted by [DJKed]. Specifically, the authors investigate the two most used network simulators, Veins (linked to OMNET++) or NS-3. The paper surveys the capabilities and employed propagation models. A head to head comparison of the two simulations reveals discrepancies in the results and caution to use them without further thought.

Finally, the last documents treat the challenging task of interfacing the real world with simulations. In the Veneris framework [ELLPGMGP19], OMNET++ is used as basis for a network simulator and generator. This is interfaced with the Unity game engine, to provide physically accurate simulation facilities. Through Unity, a 3D environment that reproduces real-world traffic dynamics, a ray-launching propagation simulator and bidirectional interfaces are implemented. It furthermore supports accurate driver behavior and vehicle models. The article discusses validation of the vehicle dynamics, the recreation of traffic flows, and the accuracy of the propagation simulations.

In the framework called Testing Environment for Vehicular Applications Running with Devices in the Loop (TRUDI) [MMC+ed] vehicles will be equipped with short-range wireless technologies with the aim to improve safety and traffic efficiency. Novel applications are thus being implemented for future cars and trucks, and one of the main issues is how to conduct tests and optimizations in an effective way, limiting the need to perform costly and time consuming experiments on the road. To cope with this issue, a simulator with hardware in the loop, called TRUDI, has been implemented. The aim of this new platform, illustrated in Fig. 7.12, is to provide a flexible solution to test V2X applications with real wireless communication devices in the loop. Starting from a logical separation of the communication device, called intelligent transport system station (ITS-S), from the processing and visualization unit,

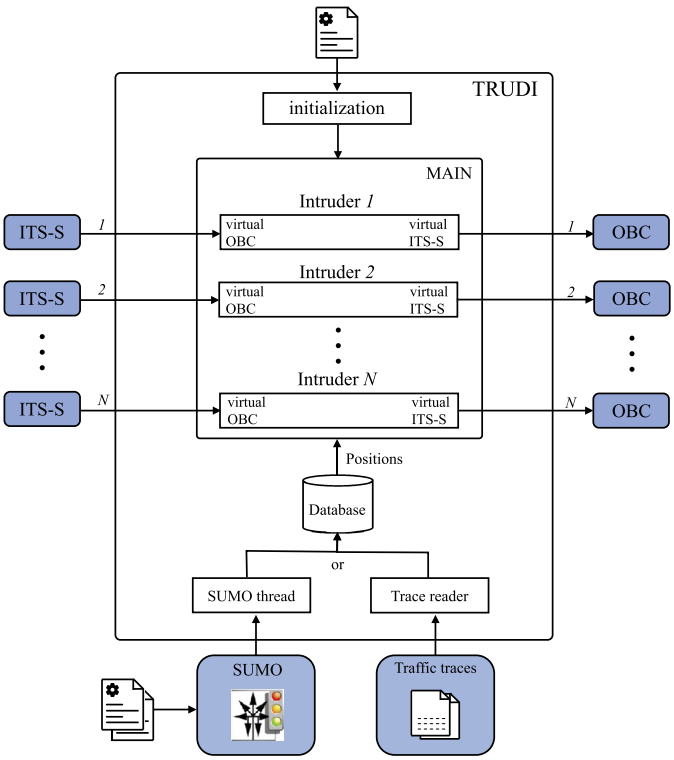

FIGURE 7.12

The internal structure of TRUDI.

denoted on-board computer (OBC), the idea is that TRUDI works in the middle of the two layers, with a man-in-the-middle approach. During the simulation, TRUDI modifies the exchanged information in order to simulate given positions and trajectories of the vehicles and to reproduce inaccuracies in the communication, such as message losses or errors in the localization. Once the application is tested, TRUDI is removed, the hardware is mounted on-board of the vehicle, and the application is ready to run. As an added value, a simulation of the ITS-Ss is also possible. As an example use case, an application for the intersection management has been implemented and tested, where the driver is warned of the presence and speed of other vehicles approaching the same junction. Once validated with TRUDI, the application was also verified on the road with real vehicles.

This approach allows for a very detailed analysis of the observed link-to-link performance. On the other hand, [BGB+19] aims at measuring in hardware the performance in a dense urban environment. The goal of the paper is to accurately assess the achievable performance for ad-hoc schemes in dense urban networks, where interference plays an important role as limiting factor. Historically, such analysis strongly

simplifies the physical layer. Instead, the goal here is to keep the complexity of the physical layer, and simplify elsewhere. The paper approaches this problem by using mobility simulators to generate vehicular positions, and then model the communication between the vehicles through a graph. Hence, the authors simplify the graph while maintaining the essential communication behaviors and statistics. This simplification shows that the presented scenario can be modeled sufficiently accurate with a very low number of devices. Hence, three transceivers and two vehicular channel hardware emulators are connected to provide performance analysis of the presented network.

7.4 Energy efficient/constrained solutions for IoT

Recent advancements in wireless networking, microfabrication and embedded microprocessors have enabled a production of massive-scale wireless nodes suitable for a range of innovative applications. Size and cost constraints on individual wireless nodes result in corresponding constraints on available resources such as energy, memory, and computational capabilities. One of the main concerns is energy consumption, since distributed wireless nodes are mainly battery operated.

7.4.1 Energy efficiency in IoT

Many solutions for IoT are using the 2.4 GHz Industrial, Scientific, Medical (ISM) band (see, e.g., IEEE 802.15.4), which usually becomes crowded because of many radio technologies sharing this band, e.g., Wi-Fi, Bluetooth, and cordless phones. Interference impacts not only the QoS and reliability of communications, but also the energy consumption of the node, because packets need to be re-transmitted. [TIPV+16] reports about some experiments carried out to characterize the impact of interference on energy consumption. As primary network two IEEE 802.15.4 devices (WSN430 nodes, using the CC2420 radio), were considered; then up to other three devices, belonging to another network, have been added progressively to create interference. Experiments were conducted into an anechoic chamber (ideal case) and into an office (real case); in both cases the distance between the transmitter and receiver nodes was 3.5 meters, whereas the interfering nodes were deployed near the transmitter (at a distance of 20 centimeters), in the ideal case, and in different places between the two nodes, in the real case (see Fig. 7.13). Interfering nodes generated packets of 100 bytes of payload every 10 ms, causing serious interference on the channel. The average energy consumed at the transmitter side, as a function of the Receiver Signal Strength Indicator (RSSI) value measured at the receiver (being an estimation of the interference level), is shown in Fig. 7.14 for the ideal case. Results demonstrate that the average energy consumed varies according to the level of interference on the channel. Moreover, a packet transmitted with an interference level situated in the slice [-75, -70] dBm will consume 4.6 times more on average than a packet sent when the RSSI value does not exceed -85 dBm. As for the real case

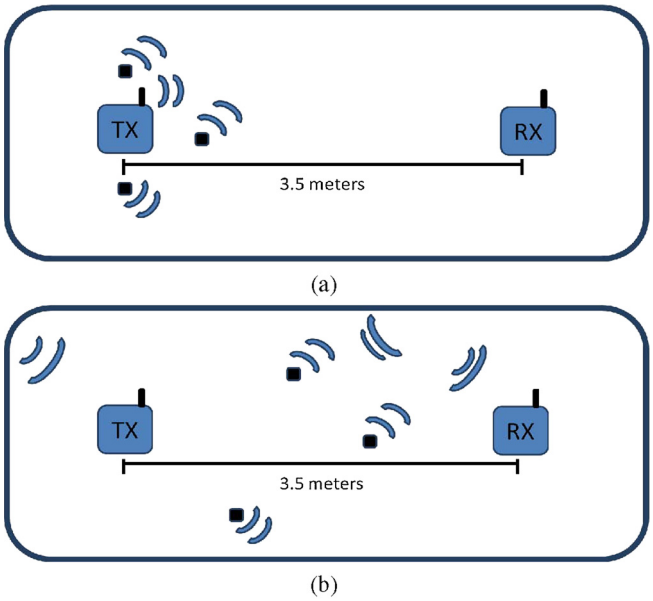

FIGURE 7.13

Scenarios of the experiment: a) in anechoic chamber, b) in office-type lab environment.

scenario (we refer to [TIPV+16] for the related results), a more significant variance of RSSI values than in the ideal case has been observed, due to presence of signal reflections and external sources of interference that could not be controlled.

It is well known that during a radio transmission, the most energy greedy part is the radio front-end. Methods to optimize the energy consumption by turning off this interface when unused have already been proposed and implemented. This could be directly managed by the hardware, adding a wake-up radio module in the transceiver [HKVG16]. The wake-up radio module has the energy consumption considerably lower than the one of the main radio front end. It will decide to activate the main radio front-end only if there is a communication demand. In Fig. 7.15, the global structure of the proposed wakeup radio receiver is presented. This receiver has two main paths. After the antenna, the signal is equally split in two branches by a power splitter. The upper branch, denoted direct path, is composed of a bank of N bandpass filters $D_1, D_2, \ldots D_N$ having the frequency shape identical to the identifier. It is also composed of an energy detector which provides V_{DC1} DC voltage, proportional to the V_{RF1} voltage at the output of the filters bank. The lower branch, denoted complementary path, is globally the same, but starting with a filter bank $C_1, C_2, \ldots C_N$ which is the exact complement of the one in the direct path. The V_{DC2} voltage at the output of the energy detector on the complementary path is subtracted from V_{DC1} and then the subtraction result is compared to a threshold by the means of a Schmidt trigger.

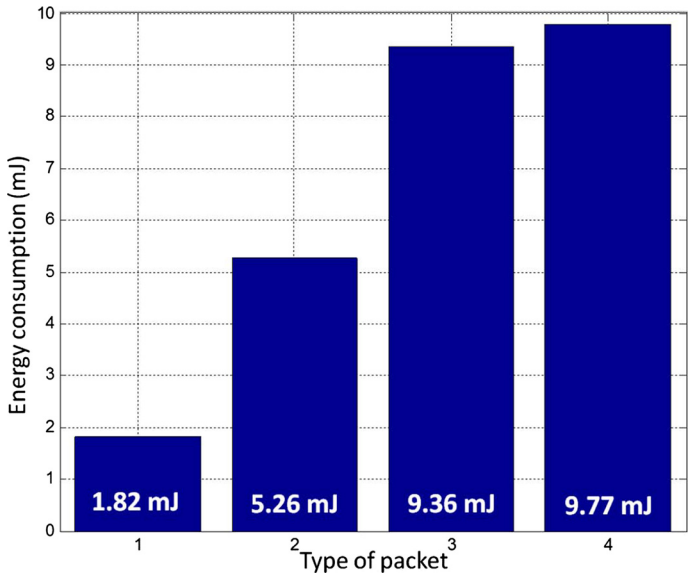

FIGURE 7.14

Energy consumption at the transmitter side versus average RSSI measured at the receiver.

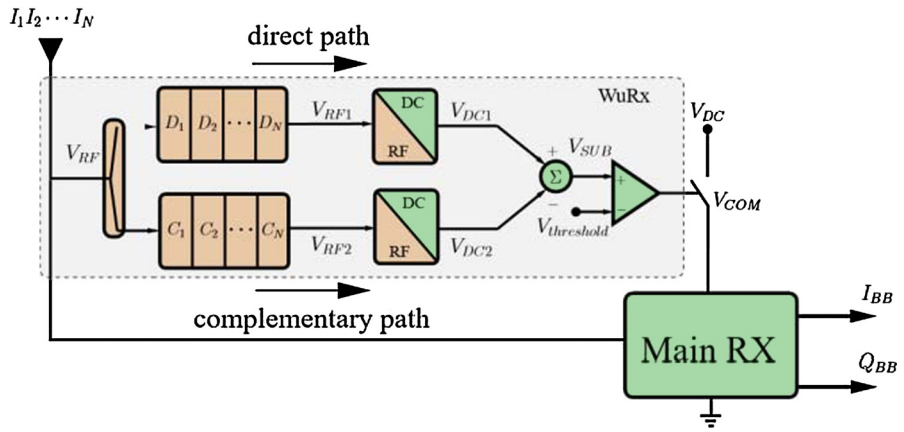

FIGURE 7.15

The wakeup radio architecture.

7.4.2 Energy harvesting aspects

Energy Harvesting (EH) has emerged as a technology capable of allowing network nodes to replenish their batteries using environmental energy sources such as, solar radiation, radio waves, or vibration. This, in turn, potentially allows the network nodes to operate for an infinite lifetime. However, the intermittent and random na-

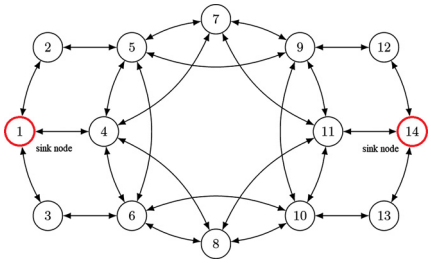

FIGURE 7.16

Example of a communications network.

ture of the energy supply makes it necessary to take a new approach to the design of communication policies. This has led to a great deal of research interest in EH-powered communication, with problems ranging from throughput maximization, source-channel coding, estimation, and others. A problem that often arises in IoT (and, in general, wireless) networks is that of routing information through the neighboring nodes. This problem was studied in [CAMR18] where the Authors proposed a joint routing and scheduling policy for data packets in an EH network. As Fig. 7.16 illustrates, each node independently generates traffic for delivery to a specific destination and collaborates with the other nodes in the network to ensure the delivery of all data packets. In this way, each node decides the next suitable hop for each packet in its queue (routing), and when to transmit it (scheduling). The solution to this problem when the nodes are not EH-powered is given by the BackPressure (BP) algorithm. By leveraging stochastic dual descent methods, the Authors proposed a generalization of the BP algorithm, referred to as EH-BP, which also accounts for the random nature of the energy supply. They also showed that the joint routing and scheduling satisfies the fundamental property of BP-type algorithms. Namely, if given data arrival rates can be supported by given energy arrival rates and some routing-scheduling policy, they can be supported by the EH-BP policy too. This extent is illustrated in Fig. 7.17 which shows a sample path of the total number of packets queued in the network at each time slot (it corresponds to the network scenario of Fig. 7.16, with nodes 1 and 14 acting as sink nodes). Average values are shown in dashed lines. As expected both the EH-BP and BP policies stabilize the queues. Nonetheless, an increase in the variance of the queue dynamics as well as the average number of packets in the network can be observed for the EH-BP policy. This is due to the random nature of the energy harvesting process. However, the average number of packets in the queues can be traded-off against the capacity of the battery (i.e., the larger the battery capacity, the lower the number of packets in the queues).

A different system scenario is addressed in [CFMAHR17]. In this work, the Authors focused on wireless networked control systems that, with the advent of Industry 4.0, are rapidly becoming prevalent. They are present in smart homes, robotic automation, smart transportation, industrial plants, and more. A critical component of these wireless control systems are the sensing devices. These sensor nodes measure

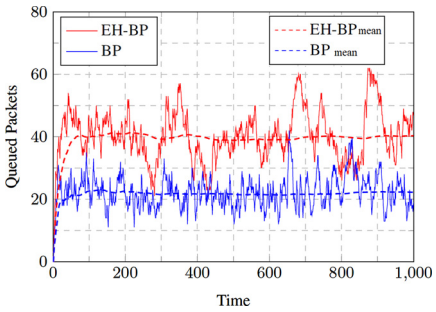

FIGURE 7.17

Number of packets queued in the network over time.

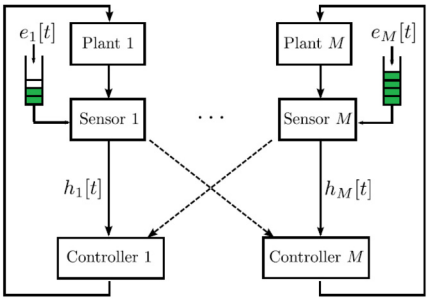

FIGURE 7.18

A wireless networked control system with EH sensors.

the state of the system and transmit their observations over a wireless channel (see Fig. 7.18). However, due to the uncertain nature of the wireless channel, the choice of communication policy critically affects the closed loop performance of the controlled systems. The sensors share the wireless communication medium and therefore one should aim for an efficient use of this resource (i.e., by avoiding packet collisions) in a way that meets the control performance requirements. Hence, the goal of this work was to design a decentralized random access policy such that all control loops satisfied their control performance requirements and the power consumption satisfied the energy causality constraints imposed by the EH process. The Authors proposed a simple dynamic threshold scheduling policy and, further, they computed the optimal scheduling policy by means of a stochastic dual method. The evolution of the control system performance (two-loop case) is shown in Fig. 7.19. Here we observe that the resulting random access policy is able to stabilize both systems since the averaged value of the state variables $x_i(t)$ asymptotically tends to a limiting value.

The work in [RDJK19] addressed the very complementary topic of Simultaneous Wireless Information and Power Transfer (SWIPT) in IoT networks. Specifically, the authors introduced a novel architecture called Modulation Split-based SWIPT. The

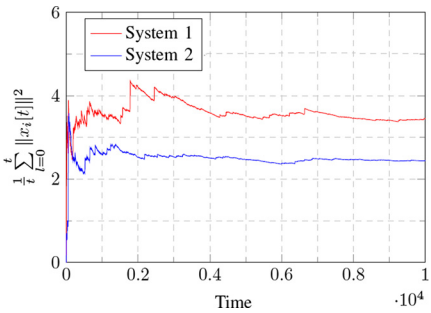

FIGURE 7.19

Evolution of the control system.

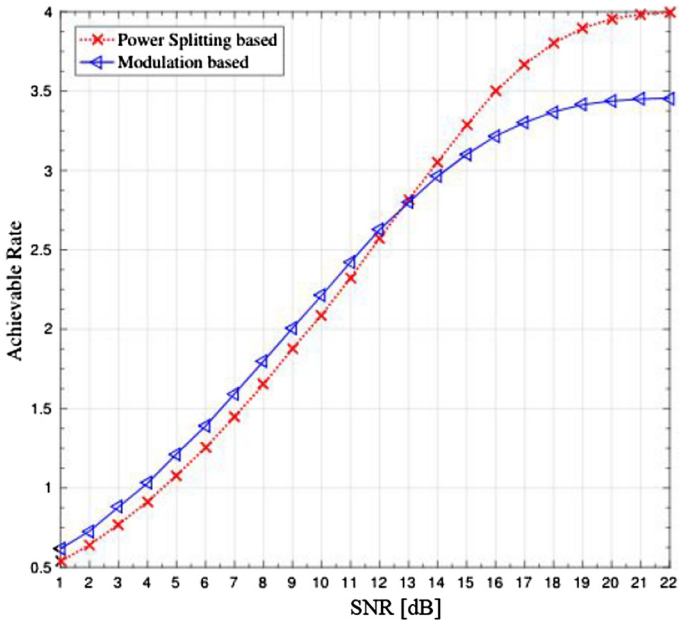

FIGURE 7.20

Achievable rate for the Modulation Split and PS schemes.

main idea here is to use specific constellation points for EH, and the rest for information transmission. This technique differs from traditional Power Splitting (PS) and time switching architectures which suffer from power losses at the symbol level. The achievable rate of Modulation Split approaches is expected to be lower than other PS schemes but QoS will not be compromised because, unlike in PS, the symbols allocated for IT do not carry power for EH. This extent is illustrated in Fig. 7.20 which reveals that Modulation Split outperforms PS in the (realistic) mid- to low-

SNR regime, whereas the situation is just the opposite for very high values of the SNR.

7.5 SDN and NFV for IoT

The use of SDN principles in IoT should enable the natural integration into future 5G wireless networks. Several research activities have been devoted to the design of SDN solutions for IoT. To validate their proposals, various prototypes have been developed and evaluated. In this section, we start by reviewing the efforts made in the definition of a SDN protocol architecture for IoT. In the second part, we present different proof-of-concept systems aiming at developing gateways allowing the communication between different IoT technologies; in these works both, the concept of SDN and SDR are exploited. We conclude the section with the topic of virtualization of IoT networks.

7.5.1 Software-defined IoT networks

A research activity has been dedicated to the design and test via experimentation of an SDN-based architecture for IoT networks.

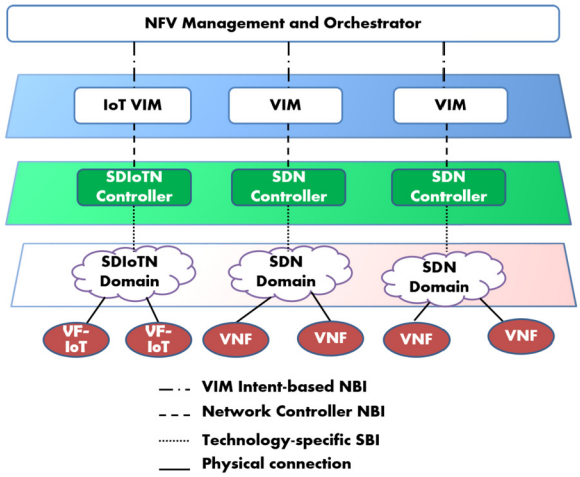

FIGURE 7.21

The general SDN-based architecture.

The proposed architecture is reported in Fig. 7.21 [CBC+17,DCT+18]. It is based on the principles of the ETSI NFV MANagement and Orchestration (MANO) framework, where high-level components, such as the orchestration layer, are in charge of managing the end-to-end network function life cycle and orchestrating the re-

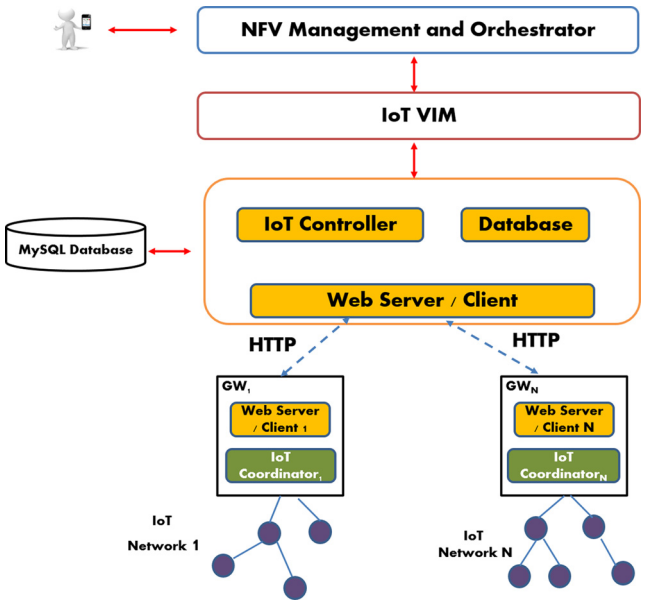

FIGURE 7.22

The Software-Defined IoT Architecture.

sources required to deploy a given service. The orchestration layer must then interact with domain-specific components, that in the case of the IoT domain include (see Fig. 7.22): i) *Management Plane*: IoT Virtualized Infrastructure Manager (VIM), which manages resources in the IoT domain; ii) *Control Plane*: SDN controller, responsible for proper traffic steering, contributing to the E2E service deployment across the domain; iii) *Data Plane*: IoT gateway and devices, representing the computing and networking resources to be managed and controlled by the other components.

The architecture also includes a database, containing the descriptors of all the IoT devices, including the IP addresses of the gateways enabling the connectivity of each IoT device, the services that they may provide and the related QoS that can be guaranteed. When a request comes from a user, the IoT VIM maps the incoming service request to the most suitable Virtual Network function (VNF); once having identified the best match, the controller will: i) program the selected IoT network ensuring the requested QoS requirements; and ii) forward the request to the gateway associated to the target VNF. The main novelty, w.r.t. previous works, such as [GMMP15] and [MR11], relies on the use of an IoT controller capable of programming the IoT networks responding to the QoS requirements specified by the end user.

In [DCT+18], the architecture is characterized in terms of the RTT performance metric. In particular, it is considered the setup shown in Fig. 7.23, where a user periodically asks for data measured by the three different sensor nodes connected to the

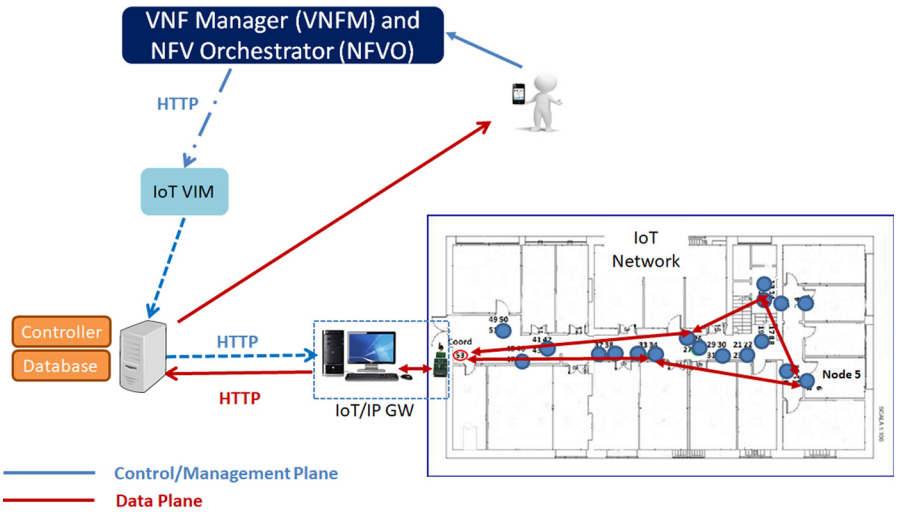

FIGURE 7.23

The Testbed Setup.

IoT network. These nodes are placed at one, two, and three hops from the coordinator, respectively. For each packet we measure: i) the RTT at the data plane, that is the interval of time between the arrival of the query coming from the controller, at the application layer of the coordinator, and the arrival of the reply from the target node, again at the application layer of the coordinator; ii) the RTT at the control plane, that is the time interval between the arrival of the query coming from the VIM, at the controller, and the arrival of the reply coming from the gateway, again at the controller; iii) the RTT at the management plane, calculated as the difference between the time stamps taken when a query arrives to the IoT VIM and when the response to the same query (if present) is sent back to the requesting user. Average RTT values are reported in Fig. 7.24. As expected the RTT slightly increases with the number of hops and when moving from data, to control, to management planes (each layer adds some processing). Results show the feasibility of the proposed solution, reporting end-to-end delays at the user in the order of 100 ms.

7.5.2 Integrating different IoT technologies

It is well known that nowadays there are many technologies available for the IoT, and there is not evidence of agreement toward one specific standard. This calls for the need of finding solutions allowing the integration of the existing technologies.

Authors of [GKAP18b] and [GKAP18a], proposed the implementation of an SDR based gateway for IoT, allowing the communication and data transfer among various networks. In particular, the gateway supports the most common short-range

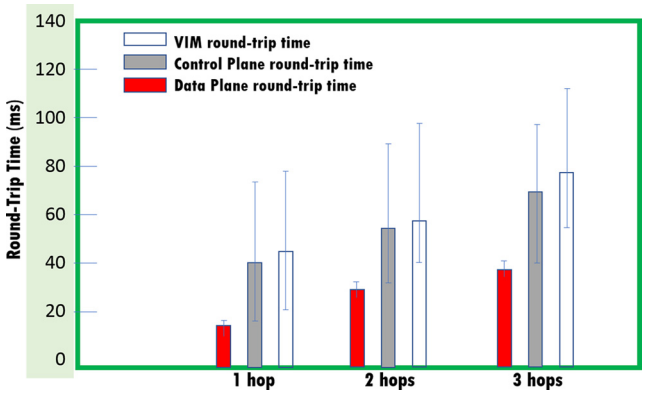

FIGURE 7.24

RTT at the different planes when considering different number of hops in the IoT network.

wireless protocols and standards, including IEEE 802.11, ZigBee, Bluetooth Low Energy (BLE), LoRaWAN, and satellite communication. SDR-based devices are able to dynamically switch between protocols and can also include spectrum sensing and packet sniffing capabilities. The first IoT gateway prototype was developed using Commercial Off-The-Shelf (COTS) radio modules. As can be seen in Fig. 7.25, four different technologies were included in the prototype. A second prototype was implemented based on the Ettus USRP310 SDR, which comprises a Zync System-on-Chip (SoC), an Field-Programmable Gate Array (FPGA), and an Advanced RISC Machine (ARM) processor. The latter prototype implemented the full protocol stacks of the IEEE 802.11g and IEEE 802.15.4 standards.

Another IoT gateway developed to create an ecosystem for overlay networks has been presented in [BRS17] and [BRS16]. The idea is to realize a mobile gateway (as shown in Fig. 7.26), enabling a reliable multi-homed communication, based on SDN concept. In particular, the gateway implements the Open Overlay Router (OOR) using the Locator Identifier Separation Protocol (LISP) protocol defined in [BRS17] and [BRS16]. The OpenDaylight SDN solution, one of the most popular SDN open-source solutions, is used to implement the controller functions. The prototype developed uses a Raspberry Pi implementation of OOR, that runs on a mobile WAN router that also includes 3G/LTE mobile connection. The mobile IoT gateway simultaneously connects different networks providing reliability and load balancing mechanisms. At the core of the WAN, the SDN controller is made available through the OOR LISPFlowMappings module. This approach opens-up new perspectives on the network management. The traffic can be steered on-the-fly based on the SDN controller OpenDayLight rules, allowing the implementation of different optimization techniques for accelerated delivery of applications or for policy enforcement, improving the IoT gateway functionality.

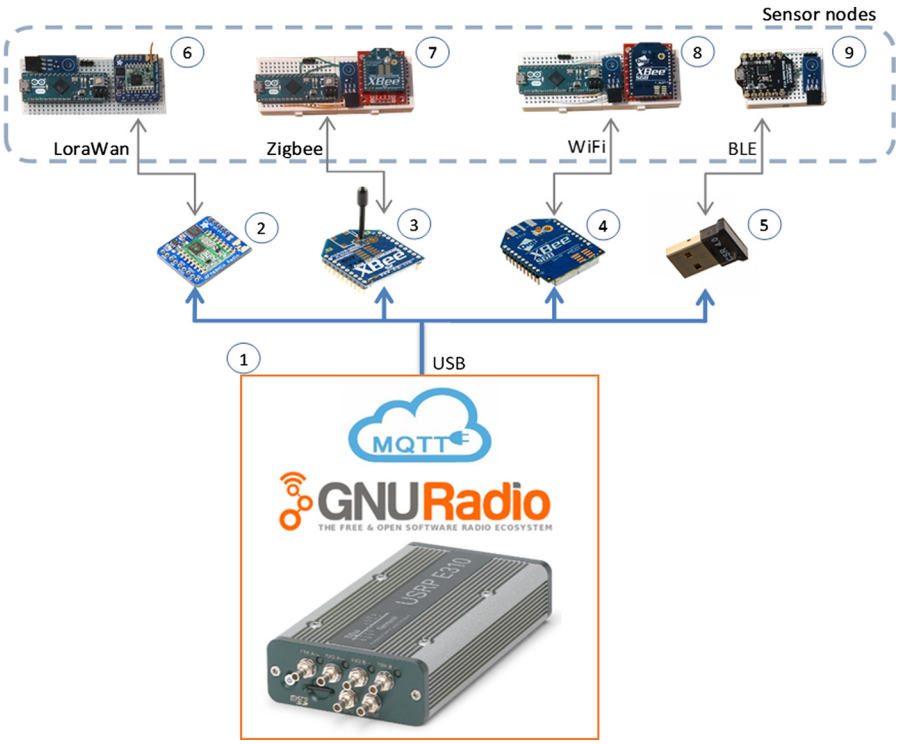

FIGURE 7.25

The architecture of proposed IoT gateway based on SDR and COTS elements.

7.5.3 Virtualization of IoT

The virtualization layer is very important for the future IoT software defined network. Thus, the authors of [DT18] examine file system performance for the native host OS performances, hypervisor-based virtualization (KVM), and container-based virtualization (Docker), based on their previous work in [TZJD17]. They have generated a workload through Filebench tool for: (1) webserver scenario dominated by random read components; (2) varmail scenario dominated by random read and random write components; and (3) file server scenario in which both random and sequential components are represented. The experiments are run for one, two, and three KVM/Docker Virtual Machines (VMs) or containers. As the number of instances increases, there is a significant drop in performance and this drop is constant on any hardware-software configuration. The Docker containers use the HostOS Fixed Service (FS) and have a small footprint and therefore have similar performances as the native host (in the case of one instance). In case of the instantiation of the container, certain performance fall will evidently occur, which is, depending on workload, slightly or strongly expressed.

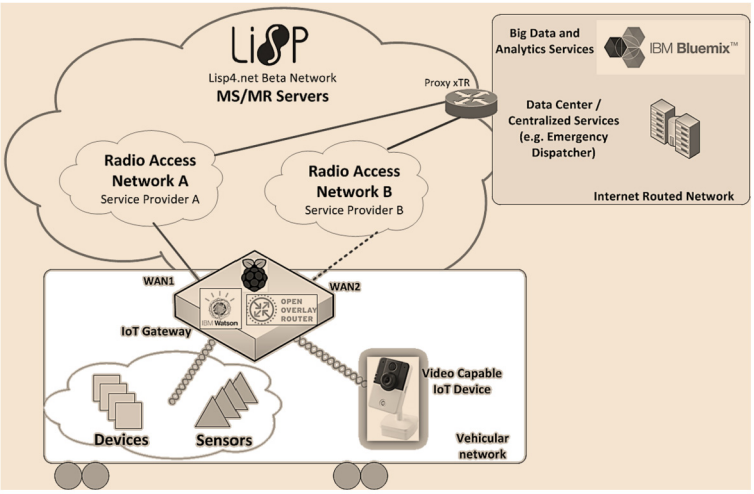

FIGURE 7.26

Scenario for a mobile IoT gateway with SDN management.

When it comes to KVM VMs, the performance drop is noticeable for the case of one VM and even more when applying larger number of VMs. Presented tests show that the Docker instance exhibits much better FS performance than KVM VMs.

An important characteristic of IoT elements is represented by the secure communication methods. Besides NFV and SDN, 5G networks envision also the implementation of Device-to-Device (D2D) communication. The ad-hoc and proximity nature of this communication introduces some very important security vulnerabilities. Key management, access control, privacy, secure routing, and transmission need dedicated signaling procedures and optimized implementation mechanisms that are appropriate for the mobile, low energy and low processing power environment. [BBS19] proposes security a mechanism for D2D communication involving the usage of physical unclonable functions (PUF) for unique key generation. Inspired by biometrics, PUFs provide a unique way to identify integrated circuits. Comparable in a simplistic way with a "unique fingerprint" of an integrated circuit, PUFs differentiate one integrated circuit from another (though apparently identical) [SCM16]. Besides the PUF unique key generation, also Elliptic-Curve Cryptography (ECC) and Diffie-Hellman Key Exchange (DHKE) are used for key management, while Salsa20/20 is the stream cyphering encryption method, suitable for confidentiality of the wireless transmissions. All these methods are implemented and tested on a SDR communication platform consisting of a Zync based SoC, complemented by RF daughter-boards from Analog Devices – an integration using hardware and software co-design.

7.6 Special applications of IoT

The IoT is the network of smart devices connected for various applications, such as process automatization and data gathering intended to simplify and secure our life. Ubiquitous sensor networks are present either in everyday life or dedicated for special applications, some of which are not seen from the consumer point of view. In this section we present some IoT solutions (either as a system or as technology components) thought for specific applications.

One of the most emerging application for the IoT is the Industry 4.0, also denoted as Factories of the Future (FoF). The concept of smart factories with advanced radio networks ensuring a reliable real-time communication was proposed at the end of 1980s [Rap89]. The main goal was to encourage commercialization and standardization of radio communication for the monitoring and controlling of machines. The shift from wired to the wireless networks dramatically helps to reduce huge capital expenditures of installation and maintenance of wires. However, the use of wireless into harsh industrial environments causes many propagation path loss issues, that must be included in the network operation analysis. The Horizon 2020 Clear5G project [htt18] envisions the FoF, where various radio technologies coexist and are converged to fulfill various QoS needs of different applications in the FoF [Zha17]. To achieve this goal, Clear5G has built a consortium with 7 partners from European Union and 5 from Taiwan, to further enhance research and international collaboration on how 5G may empower the FoF. Clear5G focuses on machine-type communications in the FoF environments employing both URLLC and mMTC services. The addressed major KPIs are consistent with the main stream of 5G development, more specifically including high density of connected devices, reaching 100 nodes per 1 m^3, low communication latency (down to 1 ms) and a high reliability (up to 99.999%) [htt18,PPP15].

Industry 4.0 scenario is also addressed in [CSM+19], where it is designed a protocol for IIoT networks, based on the 2.4 GHz LoRa technology. The protocol is based on time slots scheduling, to allow high reliability, and incorporates energy harvesting issues, since assumes nodes are charges via wireless power transfer. Through proper configuration of the so-called Spreading Factor SF parameter defined by LoRa, nodes can trade transmission ranges with achievable bit rates. It must be noticed that a proper adjustment of the LoRa physical layer parameters is required in case of coexisting with an IEEE 802.11g network, for the sake of interference mitigation.

Another interesting application refers to smart buildings and smart living. In smart buildings, one of the main challenges is the adaptation of the building's infrastructure to the network installation and operation. Such situation occurs in most cases for already constructed buildings or old ones that cannot be significantly modified. For a large-scale building, the harsh character of the environment significantly disturbs the wireless connectivity or even sometimes makes it impossible due to the high value of the path loss exponent of the radio propagation. The difficulty of changing the physical structure of a building due to technical reasons, costs or law issues implies

the investigation of alternative solutions. In [VFPK18] it was proposed to uses the ventilation network (known as Heating, Ventilation and Air-Conditioning (HVAC)). In most cases the HVAC ducts are made of metallic cylindrical elements. The propagation properties must be investigated to verify if the ventilation duct will act as cylindrical waveguide. This characterization for a typical metallic duct with diameter of 200 mm was investigated considering the following frequency bands: 433 MHz, 868 MHz, and 2.45 GHz. It was verified that the cut off frequency for the fundamental mode in such a cylindrical waveguide equals 879 MHz, which implies no occurrence of propagation modes for the 433 MHz or the 868 MHz frequency band. On the other hand, the 2.45 GHz frequency band was proposed as suitable band for applications in ducts with diameter down to 72 mm.

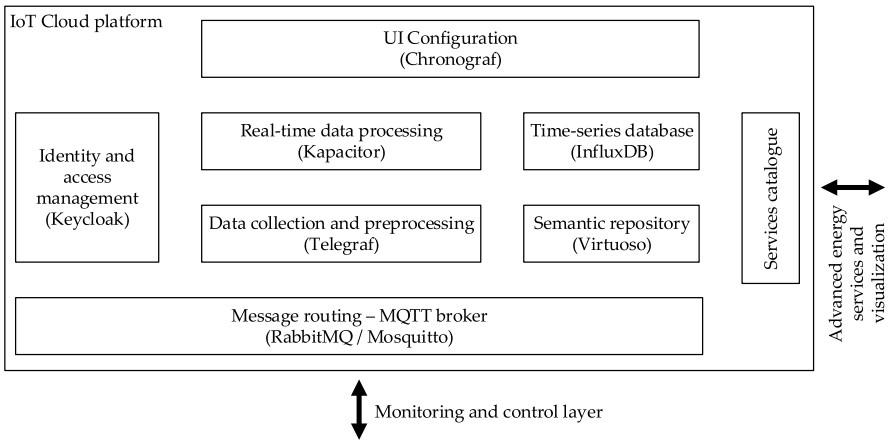

FIGURE 7.27

Cloud-based integration IoT platform for energy efficient living

Since the residential sector has been identified as one with the most demanding on energy, there exists a strong interest in exploitation of connected smart devices with the aim of improving energy efficiency, user comfort, and the overall quality of life. [BTB18] presents an IoT platform for monitoring user's energy consumption and habits with the aim of improving the energy efficiency of a household, as shown in Fig. 7.27. The platform ensures the provisioning and connection of sensors, smart meters, and actuators to the network and enables collection, processing, and exchange of data among the related components. In Fig. 7.27 the InfluxData Telegraf, InfluxDB, Chronograf, Kapacitor (TICK) Stack, composed of Telegraf (a server agent for collecting and reporting metrics), InfluxDB (a time series database for high write and query loads), and Kapacitor (a native data processing engine) were highlighted. These components can be configured and some tests can be performed in order to check sensor data acquisition, storage, and visualization through a testing Graphical User Interface (GUI). InfluxData TICK stack is an open source platform allowing users to manage metrics, events, and other time-based data.

A slightly technologically different but similar approach can be found on a Smart Campus of University of Malaga [FSRP+19]. The project Smart University of Málaga (SmartUMA) is based on four main pillars: deployment of measuring devices, setting a telecommunication networks and protocols, processing the data using the Artificial Intelligence (AI), and deploy a set of actuators. Its main goal is to improve the administration, management, and decision making at the university based on a precise knowledge of all the information that surrounds the campus.

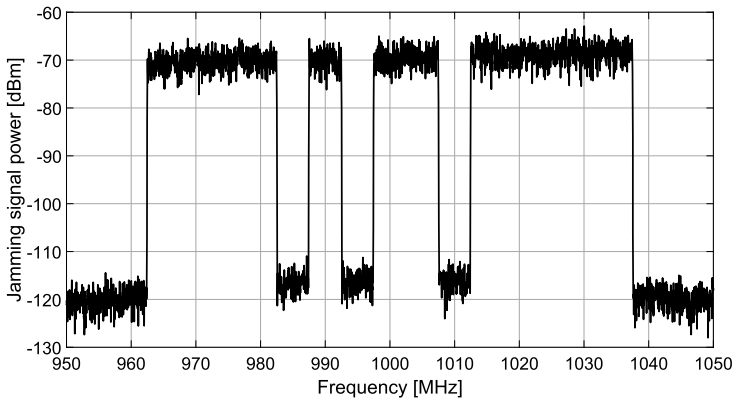

FIGURE 7.28

Spectrum of the 75 MHz width jamming signal with notched three protected bands.

Additional needs can be seen in the governmental sector. Officers of public entities like Police, Border Guard, and Army carry out their actions with left packages in different environments. Often there is a need to analyze unidentified parcels left on the airport or other public areas before their disposal. In many cases left packages are suspected to be Radio Controlled Improvised Explosive Devices (RCIEDs). To increase the security of the officers on duty and other bystanders usually some special device is used to jam radio signals that can be sent to detonate the explosives. Commonly this activity is named as setting an electromagnetic curtain. From a technical point of view, it can be understood as generating a radio signal with an occupied spectrum bandwidth of e.g. from a few MHz to hundreds of MHz. In most of the cases the jamming signal is generated in the communication bands of the cellular networks and ISM networks. In [RCM+19] such a concept is proposed, and an realization of a mobile device for generating an electromagnetic curtain is presented. The device is able to generate a wideband (with bandwidth of up to 1 GHz) jamming signal in the frequency range from 400 MHz to 2.7 GHz. The device was realized as a technological demonstrator with a size of a travel suitcase placed on a self-propelled platform. The jamming signal is generated digitally by using the software running on an ARM processor that is a part of the SoC Xilinx Zynq chip, integrating also the FPGA matrix. A unique feature of the device is that the jamming signal can be arbitrarily adjusted and generated on the basis of noise and chirp waveforms. Moreover,

certain sub-bands in the jamming signal can be notched to maintain own communication during the operation of the jammer. The example of a jamming signal is presented in Fig. 7.28.

7.7 Conclusions

This chapter has provided an overview about some recent research activities developed in the framework of the Internet of Things. It appears clearly that there is not a winner Radio Access Technology (RAT) and the Mobile Network Operators will need to be able to offer services based on a multi-RAT approach, where the best technology will be selected depending on the specific application domain. Both, 3GPP solution like NB-IoT, and non-3GPP solutions, like LoRa and IEEE 802.15.4-based solutions (e.g., 6TiSCH), will be most probably included in the future 5G ecosystem. The problem of coexistence and interoperability among these different technologies, inevitably deployed in the field, is a future research challenge.

As for the architectural viewpoint, the application of SDN and NFV paradigms to IoT is still in its infant status, but seem very promising: the definition of reliable protocols to manage networks in a centralized way, both in terms of paths definition and scheduling decisions, are still open issues, together with the definition of cross-domain and multi-modal inference and analytics for managing large scale networks. In this framework, it is expected that new machine learning algorithms, data science, and analytics will play a key role to extract value from the next generation of IoT networks.

Finally, with reference to the application domains, Industry 4.0 seems to be a very challenging and interesting field for IoT, being characterized by very stringent requirements in terms of reliability and latency; vehicular applications are also attracting much attention from both academia and industry; finally, smart environments applications, mainly with reference to smart building, city, and agriculture, are another interesting field.